Available online at www.synsint.com

Synthesis and Sintering

ISSN 2564-0186 (Print), **ISSN** 2564-0194 (Online)

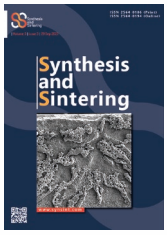

Research article

Densification-crystallization behavior of biodegradable copper-doped modified 45S5 glasses

Ahad Saeidi [a], Mojgan Heydari [b,*], Sara Banijamali [a]

[a] *Department of Ceramic, Materials and Energy Research Center, Karaj, Iran*
[b] *Department of Nano Technology and Advanced Materials, Materials and Energy Research Center, Karaj, Iran*

A B S T R A C T

In the current work, modified 45S5 glasses containing different amounts of copper oxide (1, 3, and 5 weight ratios) were prepared using melting procedure and characterized for their physical properties after sintering at various temperatures. Characterization of the copper doped glasses was performed using various analytical techniques, including X-ray diffractometry, differential thermal analysis, and scanning electron microscopy. To this purpose, a systematic study was conducted on densification-crystallization of the copper doped glasses and optimizing sintering temperature. Differential thermal analysis revealed weak exothermic peaks located above 800 °C, corresponding to the crystallization temperature (T_c) of the studied glasses. This analysis suggests that copper oxide has a limited effect on the thermal properties of the modified 45S5 glasses. Densification behavior of glass specimens was studied at temperatures ranging from 600 to 850 °C. The optimal densification temperature was found to be 650 °C, respectively. The results indicated that the presence of copper ions in the structure of studied glasses results in the formation of porous structures after sintering. It seems that copper ions generate oxygen gas during sintering and promote the formation of a cellular foam structures.

© 2023 The Authors. Published by Synsint Research Group.

KEYWORDS

Modified 45S5 glass
Copper oxide
Bioactive glass
Densification
Crystallization behavior

OPEN ACCESS

1. Introduction

Biomaterials have played a crucial role in the field of medicine for decades. These materials are designed to interact with biological systems for therapeutic or diagnostic purposes [1]. Among various types of biomaterials, ceramics have shown significant potential due to their biocompatibility, bioactivity, and mechanical properties [2]. Ceramics are inorganic materials composed of metal or non-metal atoms bonded together through ionic or covalent interactions [3]. In the biomedical field, implants, coatings, and drug delivery systems extensively utilize these materials because of their impressive mechanical and chemical stability. Additionally, ceramics possess the ability to promote tissue regeneration and healing [4]. One of the subject's undergone extensive research for biomedical applications is bioactive glass. The silicate-based bioactive glass was first introduced in the 1960s by Hench and colleagues, who discovered a particular glass composition (known as 45S5) with bone-bonding ability [5].

The composition of 45S5 glass consists of 24.5 Na_2O, 24.5 CaO, 45 SiO_2, and 6 P_2O_5 (in weight percent) [6]. The bioactivity of this glass is attributed to the ability of hydroxyapatite formation on the glass surface when it comes in contact with biological fluids, facilitating bond formation between the glass and the surrounding tissues [7]. Nevertheless, to enhance the performance of 45S5 glass in the form of scaffolds, additional adjustments are required to customize its properties for particular biomedical applications. In this regard, controlled densification of 45S5 glass powder during sintering can create intricate structures for diverse applications in tissue engineering, bone regeneration, and other biomedical applications [7].

* Corresponding author. *E-mail address:* m.heydari@merc.ac.ir (M. Heydari)
Received 5 August 2023; Received in revised form 24 September 2023; Accepted 24 September 2023.
Peer review under responsibility of Synsint Research Group. This is an open access article under the CC BY license (https://creativecommons.org/licenses/by/4.0/).
https://doi.org/10.53063/synsint.2023.33174

Despite of numerous advantages, bioactive glasses are still used restrictedly due to insufficient mechanical strength, fracture toughness, and resistance to chemical degradation [8]. To overcome these limitations, researchers have explored the addition of various metal oxides to the composition of bioactive glasses to improve targeted properties [9]. The incorporation of transition metal ions into the glass matrix is utilized to achieve such modifications, as these ions can influence the structural and compositional properties of the glass [10]. Copper is a transition metal gained considerable attention in biomedical applications due to its antibacterial properties and potential for accelerated tissue regeneration [11]. Copper oxide (CuO) has been added to the bioactive glasses to enhance antibacterial activity and accelerate hydroxyapatite formation on their surface [12]. Furthermore, CuO can promote the proliferation and differentiation of osteoblasts, which are responsible for bone formation [13, 14].

This study focuses on the preparation and characterization of modified 45S5 glasses doped with copper ions (Cu^{+}, Cu^{2+}). The main goal of this study is to explore the influence of CuO on the structure and densification-crystallization behavior of 45S5 bioactive glasses. In this regard, the synthesis process, detailed characterization, and thermal property assessment of the modified bioactive glasses are reported.

2. Experimental procedures

2.1. Material and methods

Chemical composition of starting modified 45S5 glass included 48SiO_2, 20K_2O, 18CaO, 5Na_2O, 4P_2O_5, 3B_2O_3, and 2MgO (in weight percent). The copper element was introduced into this composition in amounts of 1, 3, and 5 weight ratios in the form of copper oxide (CuO). The glass batches were prepared from reagent-grade chemicals of silica (SiO_2), phosphorus oxide (P_2O_5), calcium carbonate ($CaCO_3$), sodium carbonate (Na_2CO_3), potassium carbonate (K_2CO_3), magnesium hydroxide ($Mg(OH)_2$), and boric acid (H_3BO_3). All reagents used in the experiments were sourced from Merck, Germany.

After thoroughly mixing, glass batches were melted in an electric furnace at 1350 °C for 2.5 h using fused silica crucibles. Subsequently, the molten glasses were rapidly cooled in a water bath to obtain frits. The as-received frits were dried and then ground using an electric agate mortar for 1 h to reach a glass particle size of less than 45 µm. To fabricate glass pellets, the glass powders (< 45 µm) were homogeneously mixed with 0.5 wt% PVA solution as the binder. These mixtures were then uniaxially pressed under a pressure of 60 MPa into discs with 12 mm in diameter and 3 mm in height.

To evaluate the sinter-ability of the studied glasses, they were subjected to heat treatment at different temperatures using a heating rate of 10 °C/min. They were soaked at the maximum temperature for 1 h and then were allowed to naturally cool down to room temperature.

2.2. Characterization

To ensure amorphous inherence of fabricated frits and identify crystalline phases formed during heat treatment, an X-ray diffractometer (XRD, Philips) equipped with a cobalt lamp (k_α = 1.78 Å) was employed. The glass powders were examined by a differential thermal analyzer (DTA, Polymer Laboratories) to determine both glass transition (T_g) and crystallization (T_c) temperatures. These characteristic temperatures play a crucial role in identifying the optimal temperature range of sintering. In this test, alumina powder served as the reference sample at a rate of 10 °C/min in the air atmosphere.

After densification-crystallization heat treatment of glass compacts in the temperature range of 600–850 °C, sinter-ability parameters (including linear shrinkage, water absorption, and bulk density) were measured at each temperature, separately.

Microstructural features of sintered specimens were observed by the field emission scanning electron microscope (FESEM, TESCAN-MIRA3). Before this test, a thin layer of gold was sputtered on the surface of the samples.

3. Results and discussion

Fig. 1 illustrates the X-ray diffraction analysis of the glass powders, revealing amorphous patterns without any discernible crystalline phases. The broad diffraction peaks observed in all samples correspond to the amorphous nature of the studied glasses. It seems that the incorporation of copper ions into the glass composition did not induce the formation of any crystalline phases within the glass matrix. This result is consistent with prior research on copper-doped bioactive glasses [15, 16].

In Fig. 2, the DTA curves of the 45S5-Cu glasses in their as-fabricated state are presented. The corresponding values for the characteristic temperatures of glass transition (T_g) and crystallization peak temperature (T_c) can be found in Table 1.

The characteristics of bioactive glasses, including parameters such as the glass transition temperature (T_g) and crystallization temperature (T_c), have a profound impact on their performance as biomaterials. The temperature marked as T_g represents the point at which the glass undergoes a transition from a rigid to a more pliable state, thereby influencing both the processability and mechanical properties of the material [17]. On the other hand, T_c corresponds to the crystallization peak temperature, which affects the stability and bioactivity of the glass [18].

The DTA curves of the copper-doped glasses exhibit a subtle peak in the temperature range of 530–580 °C, which corresponds to the glass transition temperature (T_g) of the glasses. Notably, the T_g values of the copper-doped glasses closely resemble those of the undoped 45S5 glass, as shown in prior research [19].

In the case of the 45S5-5Cu variant, there is a reduction in T_g and compared to the base sample. However, for glasses with lower copper concentrations, the DTA results show no significant alterations concerning this temperature. The DTA results suggest that CuO dopants have a limited impact on the thermal properties of the 45S5 bioactive glass but may have influenced the nucleation and growth of crystals during the heat treatment [20].

As depicted in Fig. 2, by the addition of copper to the base glass, the glass transition temperature initially increases and then decreases, indicating a dependence of copper's role in the glass structure on its content. Continuous decrease of T_g values of copper-doped glasses means that their viscosity declines with the increase of copper content in the glass composition. It is worth mentioning that the T_g of a glass material affects its structure, solubility, and degradation behavior. A lower T_g value is associated with a more open structure, higher solubility, and potentially faster degradation, while a higher T_g value corresponds to a more closed structure, lower solubility, and slower degradation in bioactivity assessments. Copper ions can serve as network modifiers in glasses, leading to alterations in the glass

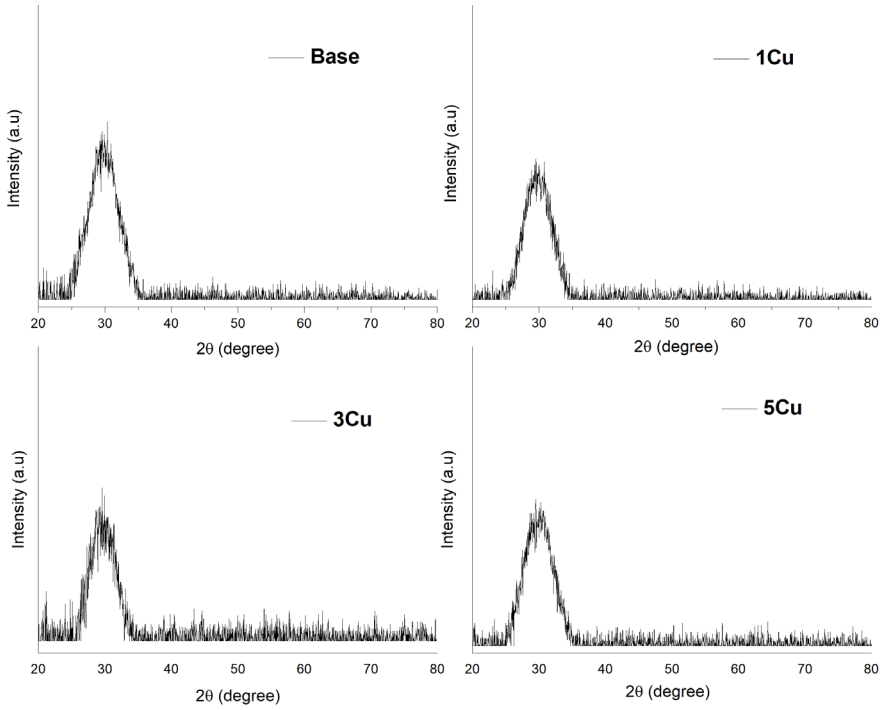

Fig. 1. X-ray diffractometry patterns of initial glass powders.

structure and shifts in T_g [21]. Generally, the addition of copper tends to lower the T_g of the glass [22, 23].

The DTA analysis also reveals that further incorporation of copper into the glass composition decreases the crystallization peak temperature. This decrease can be attributed to the disruption of the glass lattice in the presence of copper ions and lower glass viscosity. As shown in Fig. 3, wollastonite ($CaSiO_3$), pseudo-wollastonite ($Ca_3Si_3O_9$), and sodium calcium silicate ($Na_2CaSi_2O_6$) start to crystallize after 30 min heat treatment at the crystallization peak temperatures of copper doped glasses.

The sintering behavior of copper-containing samples was assessed using three parameters including water absorption, linear shrinkage,

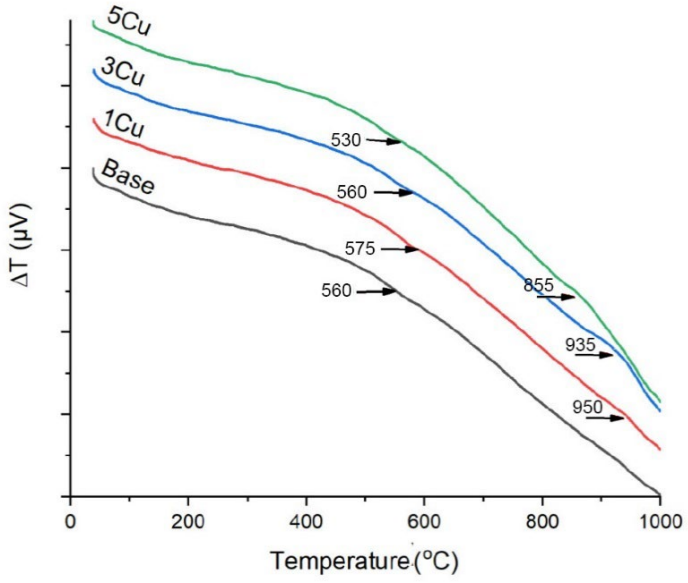

Fig. 2. DTA analysis of modified 45S5 glasses.

Table 1. Characteristic features of the examined glasses observed via DTA.

Glass	T_g (°C)	T_c (°C)
Modified 45S5	560	-
Modified 45S5-1Cu	575	950
Modified 45S5-3Cu	560	935
Modified 45S5-5Cu	530	855

and bulk density, at their respective heat treatment temperatures. Fig. 4 presents the variations of water absorption observed in the heat-treated glass samples.

As observed, the water absorption of the sintered copper-containing samples is nearly zero at temperatures exceeding 650 °C, indicating the vitrified surface of the specimens at various temperatures. The sample heat-treated at 600 °C exhibited significant water absorption, suggesting incomplete sintering.

Fig. 5 illustrates the dimensional changes and the appearance of copper-containing samples after sintering at different temperatures. Obviously, an increase in the sintering temperature initially resulted in the expansion of all samples up to 790 °C, followed by a decrease at 850 °C.

The increase in expansion observed in all samples may be attributed to the gas release resulting from oxidation and reduction reactions, along with a decrease in the surface tension of the glass. Notably, two samples exhibited shrinkage and decreased dimensions at 850 °C, which can be attributed to the gas removal from the sintered specimens. This phenomenon was particularly pronounced in the samples 1Cu and 5Cu. Visual examination of the samples sintered at temperatures ranging from 600 to 850 °C (see Fig. 5b) revealed that the dimensional change process commenced at 700 °C, while samples sintered at lower temperatures maintained their overall shape.

To assess the influence of copper on the expansion rate of the samples at different temperatures, the dimensional changes of the samples against the copper percentage have been plotted, shown in Fig. 6.

As depicted in Fig. 6, increasing the copper content at lower temperatures had no significant effect on the expansion rate of the samples. However, as the temperature was elevated to 790 and 850 °C, the copper content started to have a noticeable impact. At higher temperatures, an increase in the copper content enhanced the expansion rate, likely due to the increased oxidation and reduction of copper ions occurring at these elevated temperatures. Actually, the primary reason for the expansion of the samples is the alteration of oxidation and reduction states and changes in copper states in varying capacities.

The self-foaming effect observed during heat treatment and sintering of copper-doped bioactive glasses can be attributed to the reduction of Cu^{2+} ions to Cu^{+} ions. This process results in the production of oxygen gas (O_2) and the formation of a porous structure [24]. The Cu^{2+} ions serve as oxidizing agents and, when exposed to high temperatures, undergo a reduction reaction, accepting electrons and transforming into Cu^{+} ions. These generated Cu^{+} ions subsequently react with the surrounding silica network, leading to the breakdown of the glass network and the generation of oxygen gas.

It should be noted that by further increasing of sintering temperature, gas molecules can escape from over-sintered specimens owing to their porous structure. Consequently, the dimensions of the samples decrease at temperatures above the optimized sintering temperature. The released gas forms a cellular foam structure within the glass, which is stabilized by the remaining Cu^{+} ions within the glass [24, 25].

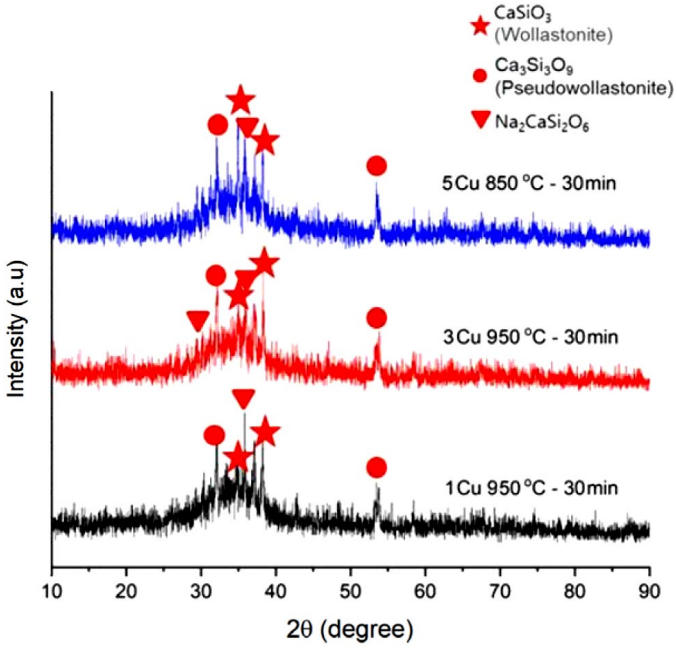

Fig. 3. X-ray diffractometry patterns of copper doped glasses heat treated at crystallization peak temperature.

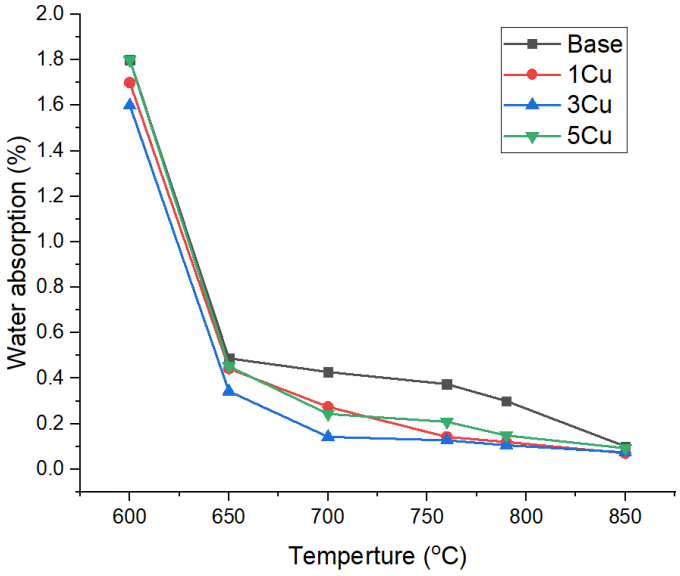

Fig. 4. Water absorption variations of examined glasses during heat treatment.

Fig. 7 shows microstructural images of the 5Cu sample heat-treated at different temperatures. Based on the findings depicted in Fig. 7, higher temperatures resulted in larger pore sizes in this specimen. Conversely, there was a tendency for the pore structure to contract. This refers to the increased pressure of oxygen gas trapped in the glass structure of high copper-containing specimens.

Fig. 8 indicates scanning electron microscope images of copper-containing samples sintered at 760 °C. As observed, with an increase in the copper percentage, the pore size increased from about 330 µm in the 1Cu sample to nearly 440 µm in the 5Cu sample.

The increase in pore size at elevated temperatures can be attributed to the increased release of gases resulting from the oxidation and reduction of copper ions at higher temperatures. This factor can lead to the formation of larger pores.

It should be noticed that the mechanism responsible for the self-foaming effect induced by copper ions in bioactive glass has remained incompletely understood. Nevertheless, several researchers have suggested that the incorporation of copper ions into the bioactive glass composition may facilitate the generation of copper oxide nanoparticles. These nanoparticles, in turn, can serve as nucleation sites during the heat treatment and sintering processes, thereby promoting the formation of gas bubbles. The generation of oxygen from the

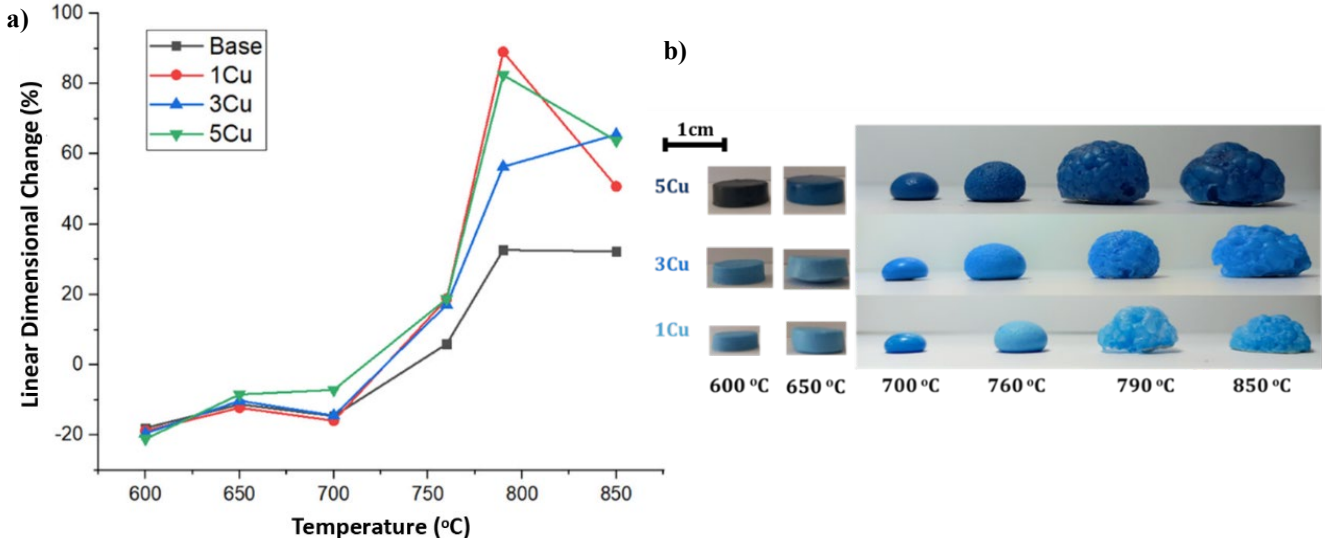

Fig. 5. Dimensional changes of copper-containing samples after sintering at different temperatures, a) variations of linear shrinkage and b) visual appearance.

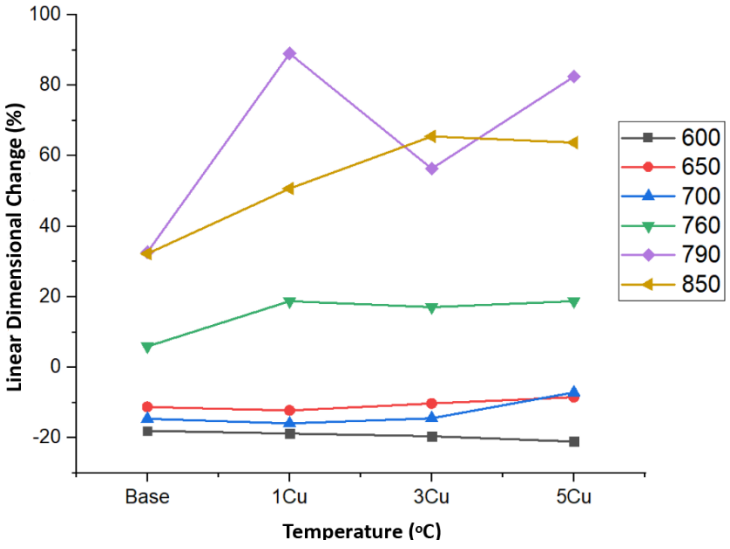

Fig. 6. The effect of copper content on dimensional changes of each specimen sintered at different temperatures.

copper oxide nanoparticles may additionally contribute to the creation of gas bubbles, further fostering the development of a cellular foam structure within the bioactive glass. Furthermore, the presence of copper ions can enhance the redox reactions occurring during the heat treatment and sintering processes, potentially augmenting the self-foaming effect [26–28].

Fig. 9 presents variations in the bulk density of copper-containing specimens at various sintering temperatures. As seen in this figure, there is an initial increase in bulk density with rising temperature, up to 650 °C, followed by a decrease at higher temperatures. This behavior closely resembles that of the original glass. Upon closer examination, it becomes evident that

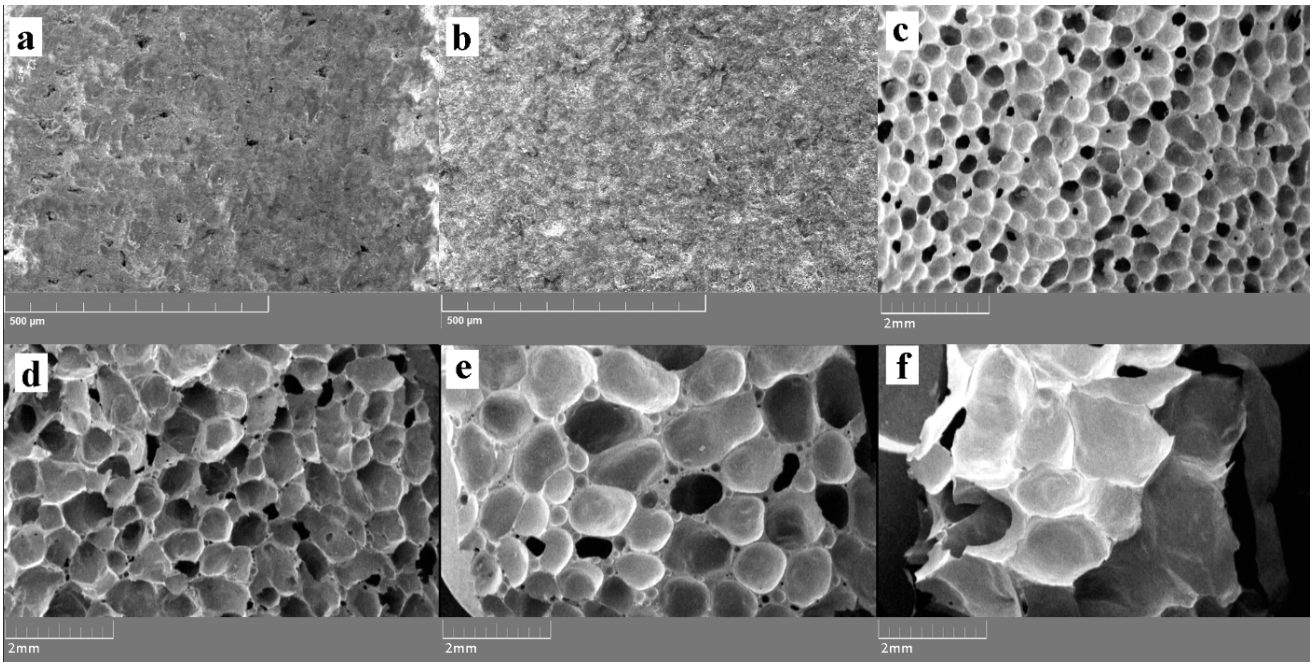

Fig. 7. Scanning electron microscope images of 5Cu specimen heat treated at a) 600, b) 650, c) 700, d) 760, e) 790, and f) 850 °C.

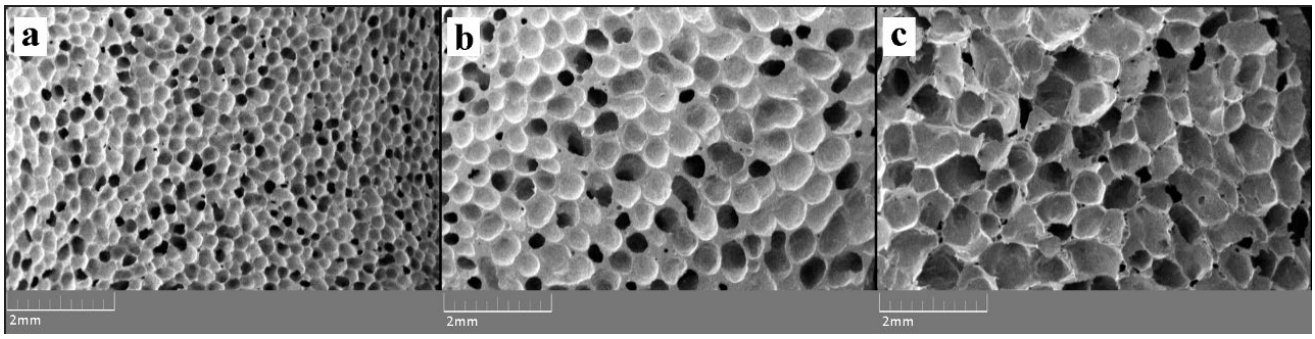

Fig. 8. SEM images of copper-containing samples sintered at 760 °C, a) 1Cu, b) 3Cu, and c) 5Cu.

the 1Cu specimen closely matches the density of the original sample. However, with an increase in copper content, the bulk density gradually diminishes. Notably, among samples sintered at different temperatures, those sintered at 650 °C exhibited higher densities.

As the sintering temperature increases, the bulk density of the sintered samples experiences a reduction. This decrease in bulk density is attributed to the formation of gas bubbles at higher temperatures during the sintering process, leading to the development of highly porous structures.

4. Conclusions

Modified 45S5 glasses containing different amounts of copper oxide were obtained using a conventional melt-quenching technique. The changes in thermal behavior induced by the addition of copper oxide to the glass composition strongly depend on the copper ion content. DTA data indicate that the incorporation of copper from 1 to 5% weight ratios decreases the crystallization temperatures of corresponding glasses. This reduction can be attributed to the disruption of the glass lattice due to the presence of copper ions which increases lattice mobility and, consequently, the crystallization rate at lower temperatures.

The addition of copper oxide to the glass composition influenced sintering behavior, resulting in the generation of oxygen gas and the formation of a cellular foam structure within the glass.

The exploration of sintering and crystallization behavior provided valuable insights into both the processing parameters and material properties of copper-doped glasses. Optimal isothermal sintering conditions were identified at 650 °C for 60 min, resulting in the lowest porosity and the highest bulk density.

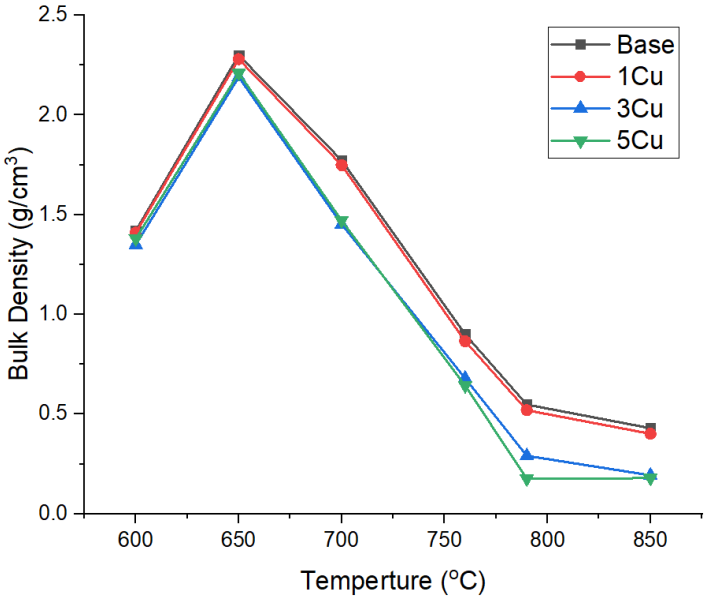

Fig. 9. Bulk density variations of copper-containing specimens sintered at various temperatures.

CRediT authorship contribution statement

Ahad Saeidi: Investigation, Formal Analysis, Methodology, Writing – original draft.
Mojgan Heydari: Supervision, Funding acquisition, Project administration, Resources.
Sara Banijamali: Supervision, Funding acquisition, Project administration, Resources, Writing – review & editing, Validation.

Data availability

The data underlying this article will be shared on reasonable request to the corresponding author.

Declaration of competing interest

The authors declare no competing interests.

Funding and acknowledgment

This project was financially supported by Materials and Energy Research Center (MERC, Iran) with project number of 381397055.

References

[1] B.D. Ratner, A.S. Hoffman, F.J. Schoen, J.E. Lemons, Biomaterials science: an introduction to materials in medicine, Elsevier. (2004). https://doi.org/10.1016/C2009-0-02433-7.
[2] L.L. Hench, Bioceramics: From concept to clinic, J. Am. Ceram. Soc. 74 (1991) 1487–1510. https://doi.org/10.1111/j.1151-2916.1991.tb07132.x.
[3] W. Lee, Ceramic processing and sintering, Int. Mater. Rev. 41 (1996) 36–37. https://doi.org/10.1179/095066096790151286.
[4] L.L. Hench, H.A. Paschall, Direct chemical bond of bioactive glass-ceramic materials to bone and muscle, J. Biomed. Mater. Res. 7 (1973) 25–42. https://doi.org/10.1002/jbm.820070304.
[5] L. Gerhardt, A.R. Boccaccini, Bioactive glass and glass-ceramic scaffolds for bone tissue Engineering, Materials. 3 (2010) 3867–3910. https://doi.org/10.3390/ma3073867.
[6] T. Kokubo, H. Hiroaki, How useful is SBF in predicting in vivo bone bioactivity?, Biomaterials. 27 (2006) 2907–2915. https://doi.org/10.1016/j.biomaterials.2006.01.017.
[7] P. Sepulveda, J.R. Jones, L.L. Hench, Bioactive sol-gel foams for tissue repair, J. Biomed. Mater. Res. 59 (2002) 340–348. https://doi.org/10.1002/jbm.1250.
[8] G. Kaur, O.P. Pandey, K. Singh, D. Homa, B. Scott, G. Pickrell, A review of bioactive glasses: Their structure, properties, fabrication and apatite formation, J. Biomed. Mater. Res. A. 102 (2014) 254–274. https://doi.org/10.1002/jbm.a.34690.
[9] F. Baino, C.V. Brovarone, Three-dimensional glass derived scaffolds for bone tissue engineering: Current trends and forecasts for the future, J. Biomed. Mater. Res. A. 97 (2011) 514–535. https://doi.org/10.1002/jbm.a.33072.
[10] H.R. Fernandes, A. Gaddam, A. Rebelo, D. Brazete, G.E. Stan, J.M.F. Ferreira, Bioactive glasses and glass-ceramics for healthcare applications in bone regeneration and tissue engineering, Materials. 11 (2018) 2530. https://doi.org/10.3390/ma11122530.
[11] H. Palza, Antimicrobial polymers with metal nanoparticles, Int. J. Mol. Sci. 16 (2015) 2099–2116. https://doi.org/10.3390/ijms16012099.
[12] D.A. Perez, R. Vargas-Coronado, J.M. Cervantes-Uc, N. Rodriguez-Fuentes, C. Aparicio, et al., Antibacterial activity of a glass ionomer cement doped with copper nanoparticles, Dent. Mater. J. 39 (2020) 389–396. https://doi.org/10.4012/dmj.2019-046.
[13] Y. Li, D. Yang, J. Cui, Graphene oxide loaded with copper oxide nanoparticles as an antibacterial agent against Pseudomonas syringae pv. Tomato, RSC Adv. 62 (2017) 38853–38860. https://doi.org/10.1039/c7ra05520j.
[14] P. Wang, Y. Yuan, K. Xu, H. Zhong, Y. Yang, et al., Biological applications of copper-containing materials, Bioact. Mater. 6 (2021) 916–927. https://doi.org/10.1016/j.bioactmat.2020.09.017.
[15] V.K. Vyas, A.S. Kumar, S. Prasad, M. Ershad, S.P. Singh, R. Pyare, Preparation and characterization of cobalt oxide doped 45S5 bioactive glass-ceramics, Innov. Corros. Mater. Sci. 5 (2015) 86–92. https://doi.org/10.2174/2352094905666150807002628.
[16] L. Mojtabavi, A. Razavi, The effects of copper addition on the structure and antibacterial properties of biomedical glasses, Eur. Chem. Bull. 9 (2020) 1–5. https://doi.org/10.17628/ecb.2020.9.1-5.
[17] M.N. Rahaman, Ceramic processing and sintering, CRC Press. (2003). https://doi.org/10.1201/9781315274126.
[18] J.R. Jones, Review of bioactive glass: from Hench to hybrids, Acta Biomater. 9 (2013) 4457–4486. https://doi.org/10.1016/j.actbio.2012.08.023.
[19] E. Fiume, J. Barberi, E. Verné, F. Baino, Bioactive glasses: from parent 45S5 composition to scaffold-assisted tissue-healing therapies, J. Funct. Biomater. 9 (2018) 24. https://doi.org/10.3390/jfb9010024.
[20] L.L. Hench, J. Wilson, Surface-active biomaterials, Science. 226 (1984) 630–636. https://doi.org/10.1126/science.6093253.
[21] A.A. Soliman, I. Kashif, Copper oxide content dependence of crystallization behavior, glass forming ability, glass stability and fragility of lithium borate glasses, Phys. B: Condens. Matter. 405 (2010) 247–253. https://doi.org/10.1016/j.physb.2009.08.154.
[22] U.G. Issever, G. Kilic, E.R. Ilik, The impact of CuO on physical, structural, optical and thermal properties of dark VPB semiconducting glasses, Opt. Mater. 116 (2021) 111084. https://doi.org/10.1016/j.optmat.2021.111084.
[23] R.M. Ramadan, A.H. Hammad, A.R. Wassel, Impact of copper oxide on the sructural, optical, and dielectric properties of sodium borophosphate glass, J. Non-Cryst. Solids. 568 (2021) 120961. https://doi.org/10.1016/j.jnoncrysol.2021.120961.
[24] F. Baino, S. Hamzehlou, S. Kargozar, Bioactive glasses: where are we and where are we going?, J. Funct. Biomater. 9 (2018) 25. https://doi.org/10.3390/jfb9010025.
[25] A.A. Gorustovich, J.A. Roether, A.R. Boccaccini, Effect of bioactive glasses on angiogenesis: a review of in vitro and in vivo evidences, Tissue Eng. Part B: Rev. 16 (2010) 199–207. https://doi.org/10.1089/ten.teb.2009.0416.
[26] D.S. Brauer, Bioactive glasses-structure and properties, Angew. Chem. Int. Ed. 54 (2015) 4160–4181. https://doi.org/10.1002/anie.201405310.
[27] Q. Fu, E. Saiz, M.N. Rahaman, A.P. Tomsia, Bioactive glass scaffolds for bone tissue engineering: state of the art and future perspectives, Mater. Sci. Eng. C. 31 (2011) 1245–1256. https://doi.org/10.1016/j.msec.2011.04.022.
[28] A. Hoppe, N.S. Güldal, A.R. Boccaccini, A Review of the biological response to ionic dissolution products from bioactive glasses and glass-ceramics, Biomaterials. 32 (2011) 2757–2774. https://doi.org/10.1016/j.biomaterials.2011.01.004.